

# Probing the Viscoelasticity and Mass of a Surface-Bound Protein Layer with an Acoustic Waveguide Device

K. Saha, F. Bender, A. Rasmusson, and E. Gizeli\*

University of Cambridge, Institute of Biotechnology, Tennis Court Road,  
Cambridge CB2 1QT, United Kingdom

Received November 6, 2002

The aim of this work is to quantify the viscoelastic properties and calculate the density of a protein layer deposited on a solid/liquid interface. Devices, which use shear-horizontal surface acoustic waves propagating in a waveguide configuration at 108 and 155 MHz, were employed in the detection of specific binding and adsorption of IgG antibodies to protein A modified surfaces and gold, respectively. To obtain both viscoelastic and mass information about the biological layers, each device was first calibrated to viscosity changes by introducing a series of glycerol–water solutions to the sensing surface. Via this calibration, an equivalent viscosity of 1.00–1.30 cP for IgG layers in solution was obtained. By modeling the proteins as solid noninteracting particles, the quantitative viscoelastic information was then used to calculate protein surface coverages of 10–300 ng/cm<sup>2</sup>, which was in good agreement with surface plasmon resonance measured surface coverages. Modeling results yield information about the mechanical and chemical interactions between proteins in surface layers. Furthermore, for the first time, simultaneous quantitative, real-time mass and viscoelastic information of protein layers at a solid/liquid interface was achieved by this technique.

## Introduction

Characterization of the properties of a protein layer at solid/liquid interfaces is highly significant in areas such as medical implants, food industry fouling processes, tissue engineering, and biosensors. Traditionally, scientists are studying the formation of such layers by measuring the deposited mass per unit area and, depending on the application, are optimizing the conditions for increasing or decreasing the protein concentration. A more advanced level of studying protein layers at interfaces would also include the study of the micromechanical properties of the layer and how these may change as a function of the surface properties, protein concentration, and medium composition.

Biological layers such as lipid bilayers and protein films consist of high-molecular-weight materials that exhibit stress behavior intermediate to that of liquids and elastic solids. Such non-Newtonian, time-dependent behavior of these materials to different deformation rates is known as viscoelasticity and governs the function of the biological layer in many mechanisms. Viscoelastic materials have a variety of mechanisms through which they may relax in response to a perturbing force. Chemical mechanisms include chain scission through hydrolysis and bond interchange. Physical mechanisms are related to interacting stress fields around each molecule and furthermore to conformational changes from molecular motions, such as segmental relaxations and slippage of chains past one another. Each mechanism has a characteristic relaxation time, and biological materials typically relax through a variety of mechanisms giving rise to a spectrum of relaxation times. Viscosity measurements in solution have already been used to follow conformational changes, as random polypeptides have higher viscosities than folded, globular proteins.<sup>1</sup>

A challenge is to detect all of the above relaxation mechanisms over a wide variety of biological materials,

ranging from single proteins to three-dimensional extracellular matrixes. Traditional methods to detect viscoelastic behavior of biomolecules are hydrodynamic techniques. Methods such as sedimentation, centrifugation, fluorescence, pulsed field gradient nuclear magnetic resonance, or triplet state anisotropy measure the velocity of the biomolecule dissolved in solvent in response to a force field on a nanosecond to microsecond time scale.<sup>2</sup> Such methods detect the rotation time of individual molecules freely suspended in solution. However, these methods are not easily amenable to apply to protein layers where relaxations involve more than individual protein rotation. Only recent techniques have improved these methods to quantify such relaxations occurring over extended biological materials. For example, recent work with optical tweezers<sup>3</sup> has probed viscoelasticity of three-dimensional cell-based architectures, although it has not been developed for extended planar materials. A technique that allows the monitoring of the viscoelasticity of a biological layer in contact with a solid support exploits acoustic waves.

Shear-horizontal surface acoustic wave devices have been designed, developed, and successfully tested to sense mass changes occurring in biological layers deposited on the device surface.<sup>4–7</sup> In addition, they have been shown both theoretically and experimentally to be sensitive to the bulk viscoelastic properties of the liquid in contact with the device;<sup>8</sup> however, very little work has been attempted in order to quantify the viscoelasticity of a biological layer. Quartz crystal microbalances (QCMs)

(2) Bloomfield, V. University of Minnesota, 2000; Vol. 2000.

(3) Li, Z. W.; Anvari, B.; Takashima, M.; Brecht, P.; Torres, J. H.; Brownell, W. E. *Biophys. J.* **2002**, *82*, 1386–1395.

(4) Bender, F.; Cernosek, R. W.; Josse, F. *Electron. Lett.* **2000**, *36*, 1672–1673.

(5) Gizeli, E.; Liley, M.; Lowe, C. R.; Vogel, H. *Anal. Chem.* **1997**, *69*, 4808–4813.

(6) Tom-Moy, M.; Baer, R. L.; Spira-Solomon, D.; Doherty, T. P. *Anal. Chem.* **1995**, *67*, 1510–1516.

(7) Harding, G. L.; Du, J.; Dencher, P. R.; Barnett, D.; Howe, E. *Sens. Actuators, A-Phys.* **1997**, *61*, 279–286.

(8) Kondoh, J.; Shiokawa, S. *Electron. Commun. Jpn. Part II-Electron.* **1995**, *78*, 101–112.

\* Corresponding author, email: e.gizeli@biotech.cam.ac.uk.

(1) Creighton, T. E. *Proteins: Structures and Molecular Principles*; W. H. Freeman and Co.: New York, 1984.

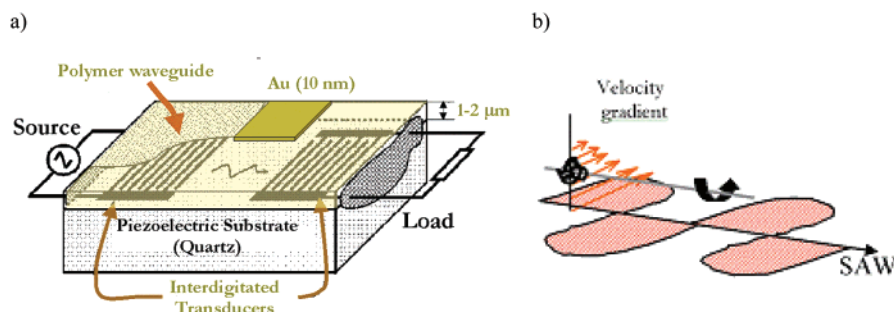


**Figure 1.** (a) Schematic of device structure. (b) Schematic of torque on molecules created by shear-horizontal surface-acoustic wave (SH-SAW) propagation in an acoustic waveguide device. Drawing not to scale.

have recently been applied to planar protein layers and lipid bilayers,<sup>9,10</sup> but the viscoelastic information obtained was not related to that obtained by other detection techniques. In addition, the device's low frequency of operation (5 MHz) results in a wave period (200 ns) of the same order of magnitude as the protein rotational relaxation time (20–10<sup>6</sup> ns). Hence, the rate of oscillation at which 5-MHz QCM devices perturb protein layers is on the time order of individual protein molecular rotation and possibly causes interference with the biological function of the protein. In this work, the capability of high-frequency acoustic waveguide devices is used to sense, in a less invasive manner, protein layer relaxations that occur in a regime that does not overlap with molecular rotation. Furthermore, viscoelastic properties of planar biological structures are quantified and related to other viscoelastic measurements.

In acoustic waveguide devices,<sup>11</sup> an electric potential applied to a piezoelectric substrate via interdigitated transducers (IDTs) creates a surface-localized, shear-horizontal acoustic wave (SH-SAW) (Figure 1a). The phase and amplitude of the SH-SAW are measured with time through electrical connections to the output IDTs. A polymer layer deposited on the device surface serves as an acoustic waveguide by localizing acoustic energy of waves in the substrate away from the bulk and onto the surface. Additional layers, such as the gold layer in Figure 1a, serve as convenient platforms to develop biorecognition surfaces. All sensing occurs in a surface layer within which there is significant acoustic displacement. Such displacement occurs when the oscillation of the device surface is coupled into the surface medium and induces an oscillation in the liquid. This oscillation does not extend throughout the bulk of the liquid but is damped within in a small distance of the surface, the penetration depth. The thickness of the penetration depth is a function of the viscosity of the surface medium and operating frequency of the device. Acoustic wave propagation is sensitive to mass, viscoelastic, and electrical changes within penetration depth.<sup>12</sup>

Viscoelastic damping of the wave creates a velocity gradient near the surface. As shown in Figure 1b, a torque arising from this velocity gradient causes rotation of suspended molecules, which in turn consumes energy. Theoretical treatment<sup>13,14</sup> of SH-SAWs predicts that the efficiency of the transmission of the wave, measured as

acoustic amplitude, should be sensitive only to viscous coupling of the surface medium for an electrically shielded propagation path. In such a system, the only means for energy dissipation of the wave is through viscous losses within the sensing volume. Phase response is sensitive to both mass and viscoelastic properties. Phase mass sensitivity has been extensively modeled and experimentally tested for a surface-attached elastic film.<sup>15</sup> The most applicable model for similar work with viscoelastic films for the acoustic waveguide device geometry includes relaxation times for a viscous liquid loaded onto the sample but has not been applied to any biological materials.<sup>14</sup>

This work is focused on using the acoustic waveguide device (Figure 1a) to measure and interpret viscoelastic changes of a surface biological layer along with mass changes. Special emphasis is made on quantifying these changes into absolute viscosities and mass surface coverages using physical models. Quartz acoustic waveguide devices at 108 MHz (Q108) and 155 MHz (Q155) were used to sense immunoglobulin G (IgG) binding and adsorption to surface immobilized *Staphylococcus aureus* protein A and gold, respectively. To obtain both mass and viscoelastic information about the two biological systems, each device was calibrated with a series of glycerol–water solutions. Via the glycerol calibration, any amplitude change seen with biological systems was correlated to an absolute viscosity of glycerol, which was termed as the “glycerol equivalent surface viscosity,”  $\eta_{\text{gly}}^s$ . Application of the Einstein relation, based on Brownian motion of solid non-interacting particles, to the  $\eta_{\text{gly}}^s$  of biological layers yielded surface mass coverages. Experimental agreement and deviation from the model generate information about mechanical and chemical surface interactions between proteins in different regimes.

### Experimental Section

**Materials.** Phosphate buffered saline (PBS) tablets, pH 7.4 (0.01 M phosphate, 2.7 mM potassium chloride, and 0.137 sodium chloride), 2-ethoxyethyl acetate, glycerol, and *Staphylococcus aureus* protein A were purchased from Sigma. Novolac photoresist was purchased from Shipley. Monoclonal immunoglobulin G (IgG), raised against hormone estrone 3-glucuronide (anti-E3G IgG), was obtained from Unilever Research, Colworth, UK.

**Devices.** (i) Q108 MHz. A 108 MHz quartz device was fabricated on a 0.5 mm thick piezoelectric quartz crystal, specifically a rotated Y-cut (42.5°) quartz with propagation 90° with respect to the *x*-axis. The interdigitated transducers (IDTs) comprised of 210-nm-thick Cr/Au (10/200 nm) electrode and consisted of 80 pairs of split fingers with a periodicity of 45  $\mu\text{m}$ . The path length of the device was 7.21 mm.

(ii) Q155 MHz. A 155-MHz quartz device was fabricated on a 0.5-mm-thick piezoelectric quartz crystal, specifically a rotated Y-cut (42.5°) quartz with propagation 90° with respect to the *x*-axis and comprised of 92 electrode pairs. The devices were

(9) Rodahl, M.; Hook, F.; Fredriksson, C.; Keller, C. A.; Krozer, A.; Brzezinski, P.; Voinova, M.; Kasemo, B. *Faraday Discuss.* **1997**, *107*, 229–246.

(10) Keller, C. A.; Kasemo, B. *Biophys. J.* **1998**, *75*, 1397–1402.

(11) Gizeli, E. *Anal. Chem.* **2000**, *72*, 5967–5972.

(12) Ballantine, D. S. *Acoustic wave sensors: theory, design, and physicochemical applications*; Academic Press: San Diego, 1997.

(13) Josse, F.; Shana, Z. *J. Acoust. Soc. Am.* **1989**, *85*, 1556–1559.

(14) McHale, G.; Lucklum, R.; Newton, M. I.; Cowen, J. A. *J. Appl. Phys.* **2000**, *88*, 7304–7312.

(15) McHale, G.; Newton, M. I.; Martin, F. *J. Appl. Phys.* Submitted 2002.

fabricated with 120-nm-thick Cr/Au (20/100 nm) split finger IDTs having a period of 32  $\mu\text{m}$ . The device utilized a dual delay line configuration where one delay line could act as the reference line and the other as the sensing line. The path length of the device was 5.73 mm.

**Instrumentation.** For the Q108 MHz device a Hewlett-Packard 4195A network analyzer was used to monitor the frequency and phase of the wave together with an HPVEE program. To minimize interfering reflections, the device was measured with scotch tape on the back. For the Q155 MHz, a Hewlett-Packard 8753ES network analyzer was used for performing the measurements together with a VEE software program for collecting data. The Fourier transform/time gating function of the device was used for biosensing measurements in order to minimize unwanted interference with electromagnetic feed-through and triple transit signals. Acoustic phase and amplitude measurements were reproducible between the two network analyzers. Surface plasmon resonance (SPR) measurements were performed by using an AUTOLAB SPR (Eco Chemie B. V., Netherlands) instrument.

**Polymer Waveguide–Novolac Deposition.** Different polymer concentrations were prepared by diluting the polymer in 2-ethoxyethyl acetate. Novolac solutions (50 and 60% w/w) were applied on the device surface by using a spin coater (Speciality Coating Systems P6700) at 4000 rpm for 40 s. The solvent was evaporated by heating the coated device in an oven at 190 °C for 2 h. The devices were measured before and after coating with the polymer and the frequency and amplitude changes were recorded. The thickness of the waveguide layer was measured to be 0.9 and 1.5  $\mu\text{m}$  by using a surface profilometer (Dektak) for 50% and 60% w/w Novolac solutions applied, respectively.

**Device Cleaning.** The Novolac-coated Q108 MHz devices were cleaned by soaking them in 4 M sodium hydroxide for at least 1 h and then placing them in a sonicating bath for 20 min in sodium hydroxide followed by distilled water rinse. The Q155 MHz Novolac coated devices were treated with sodium hydroxide solution as above and then were dipped into freshly prepared and still hot (50 °C) Piranha solution, consisting of sulfuric acid (97%) and hydrogen peroxide (27.5%) in a ratio of 3:1 (v/v), for 5 min.

**Gold Surface Preparation.** The area between the IDTs on the Novolac device was coated with 10 nm of gold by thermal evaporation at a pressure of less than  $5.0 \times 10^{-6}$  mbar by using an Edwards (Auto 306) evaporator. Plasma etching of the surface utilized atmospheric gas at  $9.0 \times 10^{-2}$  to  $2.1 \times 10^{-1}$  mbar for 5 min.

**Liquid Loading and Flow.** Each device was mounted in a special holder and the liquid was pumped through with a peristaltic pump and flow through cell. The flow cell was sealed on the surface by using a custom-made rubber gasket. Due to the different size of each device, two different flow cells were manufactured exposing 0.12 and 0.06  $\text{cm}^2$  of the Q108 and Q155 devices, respectively, to the solution.

**Glycerol–Water Solution Experiments.** The freshly prepared gold surface was placed in the device holder and exposed to water to obtain stable acoustic phase and amplitude signals. Glycerol–water solutions 10–40% (w/w solution) were passed on top of the device at a flow rate of higher than 83  $\mu\text{L}/\text{min}$ . Each application of glycerol solution was followed by a water rinse.

**IgG Binding to a Protein A Modified Device Surface.** The freshly prepared gold surface was placed in the device holder and exposed to PBS buffer for approximately 1 h at a flow rate of 83  $\mu\text{L}/\text{min}$ . Protein A at a concentration of 50  $\mu\text{g}/\text{mL}$  in PBS was added and left in contact with the device surface at the above flow rate for 30 min. Different solutions of monoclonal antibodies of anti-E3G IgG at a concentration range of 0.7–333 nM in PBS were finally added to the device surface followed by buffer rinse.

**IgG Adsorption onto a Gold Device Surface.** The freshly prepared, plasma-etched gold surface was placed in the device holder and exposed to PBS buffer for approximately 1 h at a flow rate of 60  $\mu\text{L}/\text{min}$ . Different solutions of monoclonal antibodies of anti-E3G IgG at a concentration range of 0.7–333 nM in PBS were finally added to the device surface followed by buffer rinse.

**IgG Adsorption onto Gold: Study with Surface Plasmon Resonance.** A freshly prepared, plasma-etched gold surface on

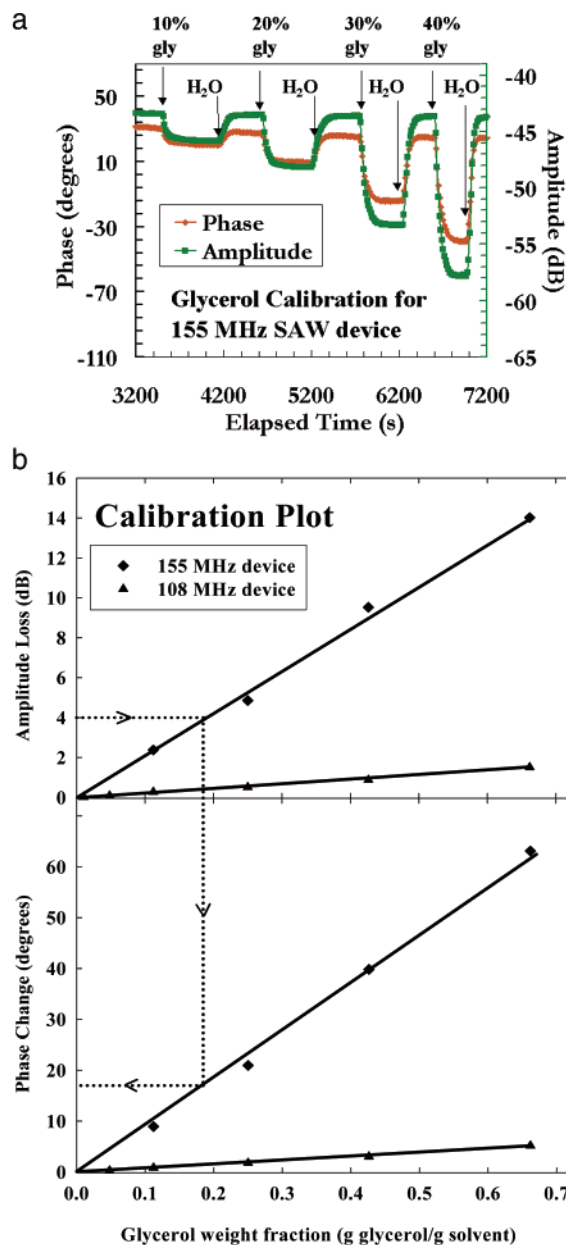


**Figure 2.** (a) Real-time data during glycerol calibration experiment for the 155-MHz device. Sequence of solutions (w/w) applied: water, 10% glycerol, water, 20% glycerol, water, 30% glycerol, water, 40% glycerol, and water. (b) Viscoelastic calibration plot for 155- and 108-MHz devices. Amplitude and phase changes seen during glycerol calibration [e.g., Figure 2(a)] are plotted here. For example, amplitude loss of 4 dB indicates 16° of phase change from viscoelasticity.

a glass slide was placed in the AUTOLAB SPR sample holder and exposed to PBS buffer for approximately 1 h in a static liquid cell. Different solutions of monoclonal antibodies of anti-E3G IgG at a concentration range of 0.7–333 nM in PBS were finally added to the device surface followed by buffer rinse and soak in PBS for 10 min.

## Results

**Calibration of Viscosity Sensitivity of each Device with Glycerol.** Introducing a series of glycerol solutions to the sensing surface provided a simple, empirical method to separate and quantify the viscoelastic response of each device. Glycerol–water solutions of different viscosities were passed on top of Q108 and Q155 devices by using a flow cell arrangement driven by a peristaltic pump. Figure 2a shows the acoustic signal in real time for the Q155

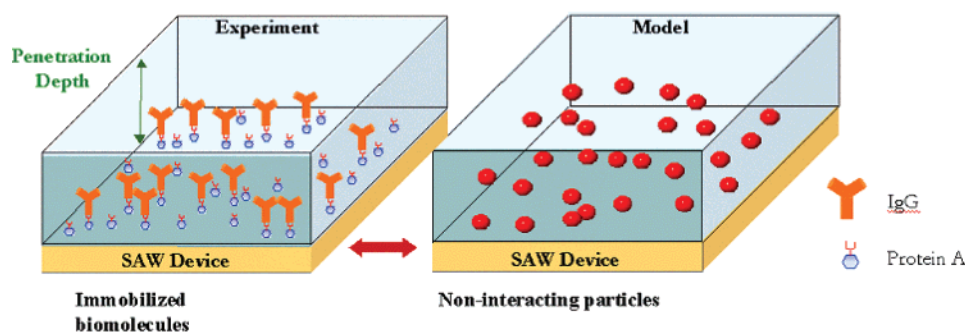


**Figure 3.** Schematic of protein layer viscoelasticity model.

device as different concentrations of glycerol–water solutions (10–40% w/w solution) were passed on the device surface, alternating with water washes. Changes in amplitude and phase of the wave in Figure 2a were considered with respect to deionized water and plotted against the glycerol weight fraction (Figure 2b). The measured loss in amplitude directly corresponds to the change in viscosity of a glycerol–water solution from that of pure water. Using a simple proportional relationship, a sensing area normalized amplitude loss,  $\Delta\text{Amp}$  is easily fit with  $w_{\text{gly}}$ , the weight fraction of glycerol, grams of glycerol/grams of solvent:

$$\Delta\text{Amp} = \frac{A_1}{\text{Area}_{\text{sensing}}} w_{\text{gly}} \quad (1)$$

where  $\text{Area}_{\text{sensing}}$  is the surface sensing area of the acoustic waveguide device and  $A_1$  is the slope of the glycerol calibration line in the  $\Delta\text{Amp}$  versus  $w_{\text{gly}}$  plot (Figure 2b). Exactly analogous fitting of phase changes was done. Figure 2b contains all the information from the calibration and can be used to correlate amplitude changes observed with this device during protein adsorption/binding to absolute viscosities.

**Quantitative Viscosity Determination of Antibody Layers—Glycerol Equivalent Surface Viscosity.** From the device calibration (eq 1), for a given any amplitude loss a “glycerol equivalent weight fraction” is determined for viscosity sensing purposes:

$$w_{\text{gly}} = \frac{\Delta\text{Amp}}{A_1/\text{Area}_{\text{sensing}}} \quad (2)$$

By use of standard viscosity data of glycerol solutions, an absolute viscosity from  $w_{\text{gly}}$  is found:

$$\eta_{\text{solution}} = \eta_{\text{water},20^\circ\text{C}} [C(w_{\text{gly}})^D + 1] \quad (3)$$

where  $C$  and  $D$  are the constants from power law fit of viscosity to the weight fraction of glycerol obtained from plotting glycerol–water CRC Handbook data,<sup>16</sup> and  $\eta_{\text{solution}}$  is the absolute viscosity of the solution. For any solution, the absolute viscosity from eq 3 is termed the “glycerol equivalent surface viscosity”,  $\eta_{\text{gly}}^s$ .

**Quantitative Viscoelastic Information from Antibody Deposition Experiments.** The glycerol calibration shown in Figure 2b was used to obtain viscoelastic information about two protein systems: IgG bound to

surface-adsorbed protein A layers and IgG adsorbed on gold. For IgG binding to protein A, the measured change in amplitude,  $\Delta\text{Amp}_{\text{IgG}}$ , directly corresponds to the change in viscosity of a phosphate buffer (PBS) + protein A + IgG solution from that of a PBS + protein A solution (data not shown). In addition, during such experiments, there is a change in amplitude associated with protein A adsorption before IgG binding (data not shown). Using eq 2, the glycerol equivalent weight fraction is obtained for both protein A addition,  $w_{\text{glyPrA}}$ , and IgG binding,  $w_{\text{glyIgG}}$ . Inserting both of these weight fractions into eq 3, the glycerol equivalent surface viscosity of the PBS + protein A + IgG solution is obtained:

$$\eta_{\text{gly}}^s = \eta_{\text{water},20^\circ\text{C}} [C(w_{\text{glyIgG}} + w_{\text{glyPrA}})^D + 1] \quad (4)$$

The viscosity of a PBS solution is assumed to be that of pure water, since the volume fraction of solutes in PBS is negligible. Calculations for IgG adsorption to gold are identical except that in eq 4  $w_{\text{glyPrA}}$  is zero. *Conceptually, adding proteins to the layer is similar, for viscoelastic purposes, to adding glycerol to the solution until it contains  $w_{\text{gly}}$  glycerol.*

**Antibody Volume Fraction Determination Using the Einstein Relation Model.** The viscoelastic effect of adding proteins to the sensing surface is modeled by applying the Einstein relation<sup>17</sup> for solid particles:

$$\eta_{\text{solutionwithparticles}}/\eta_{\text{solution}} = 1 + v\phi_{\text{particles}} \quad (5)$$

where  $v$  is the shape factor of the particle (2.5 for a sphere), and  $\phi_{\text{particles}}$  is volume fraction of the particles in the sensing volume. This relationship is valid for volume fractions less than 0.2. Treating the IgG antibodies as particles for the antibody experiments (Figure 3), the relation becomes as follows:

$$\eta_{\text{IgG+PrA+PBS}}/\eta_{\text{PrA+PBS}} = 1 + v\phi_{\text{IgG}} \quad (6)$$

Both viscosities in eq 6 are approximated through  $\eta_{\text{gly}}^s$ . Substituting expressions for  $\eta_{\text{gly}}^s$  of the protein A and IgG–protein A layers from eq 4, an explicit relationship is obtained for the volume fraction of IgG in the sensing volume:

$$\phi_{\text{IgG}} = 1/v \left( \frac{[C(w_{\text{glyIgG}} + w_{\text{glyPrA}})^D + 1]}{[C(w_{\text{glyPrA}})^D + 1]} - 1 \right) \quad (7)$$

The largest volume fraction obtained for IgG at surface saturation was 0.11, well below the 0.2 cutoff criterion for application of the Einstein relation.

(16) Weast, R., Ed. *CRC Handbook of Chemistry and Physics*, 58 ed.; CRC Press: Boca Raton, Florida, 1977.

(17) Einstein, A. *Ann. Phys. (Leipzig)* **1906**, 19.

**Surface Mass Coverage Calculation from Volume Fraction.** By definition, the volume fraction of proteins in the sensing volume depends on the number of proteins and acoustic penetration depth as follows:

$$\phi_{\text{IgG}} = \frac{n_{\text{IgG}} V_{\text{IgG}}}{\delta(\text{Area}_{\text{sensing}})} \quad (8)$$

where  $\delta$  is the acoustic penetration depth,  $n_{\text{IgG}}$  is the number of IgG molecules within the sensing volume, and  $V_{\text{IgG}}$  is the volume of individual IgG molecules. The shape of an IgG molecule is approximated as a rectangular prism with dimensions of  $23 \text{ nm} \times 23 \text{ nm} \times 4.4 \text{ nm}$ .<sup>18</sup> Using the molecular weight of IgG molecules ( $\text{MW}_{\text{IgG}} = 150\,000$ ) a mass per unit area from the volume fraction in eq 8 is obtained:

$$\frac{\text{Mass}_{\text{IgG}}}{\text{Area}_{\text{sensing}}} = \frac{\delta \phi_{\text{IgG}} \text{MW}_{\text{IgG}}}{V_{\text{IgG}} (6.02 \times 10^{23})} \quad (9)$$

**Acoustic Penetration Depth.** The acoustic penetration depth in eq 9 varies with viscosity of the solution and device frequency as follows:

$$\delta = \sqrt{\frac{\eta}{\pi f \rho_{\text{solution}}}} \quad (10)$$

where  $\rho_{\text{solution}}$  is the density of the medium above the acoustic waveguide device, and  $f$  is the frequency of the acoustic waveguide device. The density of the solution is estimated as follows:

$$\rho_{\text{solution}} = \frac{\text{Mass}_{\text{IgG in sensing area}} + \text{Mass}_{\text{water in sensing area}}}{V_{\text{total in sensing area}}} \quad (11a)$$

$$\rho_{\text{solution}} = \frac{\phi_{\text{IgG}} \text{MW}_{\text{IgG}}}{V_{\text{IgG}} (6.02 \times 10^{23})} + \rho_{\text{water}} \quad (11b)$$

Final biomass/area for IgG binding and adsorption is calculated by using eqs 2, 7, 9, 10, and 11b in combination. Results for all protein systems and devices are shown in Figure 4.

## Discussion

**Calibration of Viscosity Sensitivity of Each Device with Glycerol.** For device calibration with a series of glycerol–water solutions, the changes seen in acoustic response (Figure 2) are consistent with experimental data in the literature and theory for the low viscosity and high-frequency regime of these experiments.<sup>13,19,20</sup> The linear response of amplitude to weight fraction glycerol (Figure 2b) indicates a colligative property relationship as seen in the literature.<sup>13,19,20</sup> According to models of the device that incorporate viscous loading of the SAW device,<sup>14</sup> anomalous response should not occur from shear resonances in the penetration depth for such low viscosity solutions in the frequency range 108–155 MHz. Furthermore, the longest shear relaxation time,  $\tau$ , of the most viscous solution in the experiments is 0.07 ns for 40% w/w glycerol, as calculated by  $\tau = \eta/\mu$ , where  $\mu$  is the high-frequency rigidity modulus of  $5 \times 10^7 \text{ N/m}^2$ .<sup>13</sup> Since the

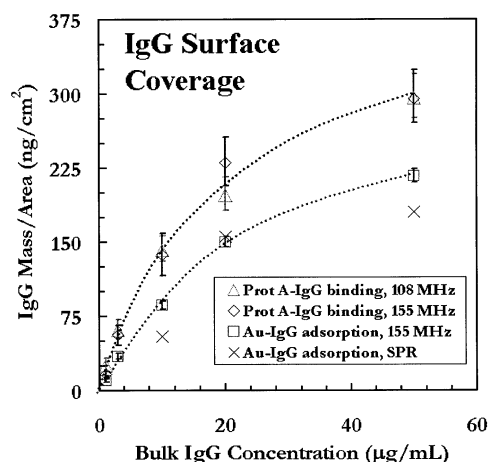


**Figure 4.** Antibody surface coverage for different bulk IgG concentrations applied to a protein A modified 108-MHz quartz device, a protein A modified 155-MHz quartz device, a 155-MHz quartz device, and a surface plasmon resonance (SPR) gold slide. Surface coverage was calculated by modeling amplitude loss during binding or adsorption. Note that these data represents an approximate adsorption isotherm, as sufficient time was not given for binding or adsorption to reach complete equilibrium. Error bars arise from modeling the random error in amplitude during binding or adsorption.

longest  $\tau$  in all of the glycerol solutions is much lower than the period of wave oscillation (6–10 ns), there are no relaxations in the low viscosity glycerol solutions that are not sensed by the device.<sup>13</sup>

A general way to illustrate the amplitude–viscosity relationship is by plotting the density-normalized amplitude change as a function of the square root of the viscosity of the liquid,  $\eta^{1/2}$ . The relationship has been predicted and demonstrated to be linear for a range of solution viscosities for the measurements made with SH-SAW devices<sup>21</sup> and acoustic plate mode devices, also operating in a shear mode.<sup>13</sup> Similarly for the phase–viscosity relationship, traditional plots show phase versus square root of the density and viscosity product. The data from Figure 2b were also plotted as  $\Delta\text{Amp}/\rho_{\text{solution}}^{1/2}$  against  $\eta^{1/2}$  and  $\Delta\text{phase}$  against  $(\eta\rho_{\text{solution}})^{1/2}$  with viscosities calculated from eq 3 (plot not shown). In such plots, although a relatively good linear relationship was seen with correlation coefficients of 0.998–0.999, there was no improvement on the linear fits with weight fraction of glycerol (grams of gly/grams of solvent), as demonstrated in Figure 2b, with correlation coefficients of 0.998–0.9999. Signal amplitude loss and phase change were therefore considered in terms of weight fraction of glycerol (grams of gly/grams of solvent).

Theoretical treatment<sup>13,14,20,22</sup> of SH-SAWs predicts acoustic amplitude to be sensitive only to viscous coupling of the surface medium for an electrically shielded propagation path. The magnitude of amplitude loss is dependent on the amount of liquid coupled to the surface oscillations. The volume of liquid depends on the penetration depth and therefore depends on the density through eq 10. This density dependence was found to be weak in the calibration, since normalizing  $\Delta\text{Amp}$  from Figure 2a by  $\rho_{\text{solution}}^{1/2}$ , consistent with eq 10 and Josse et al., and replotting it against glycerol weight fraction did not yield a better fit. Note that since these glycerol solutions are Newtonian, amplitude response was not seen to differ with varying flow rates.

(18) Golander, C. G.; Kiss, E. *J. Colloid Interface Sci.* **1988**, *121*, 240–253.

(19) Melzak, K.; Martin, F.; Newton, M. I.; McHale, G.; Gizeli, E. *J. Polym. Sci. Part B: Polym. Phys.* **2002**, *40*, 1490–1495.

(20) Ricco, A. J.; Martin, S. J. *Appl. Phys. Lett.* **1987**, *50*, 1474–1476.

(21) Weiss, M.; Welsch, W.; Von Schickfus, M.; Hunklinger, S. *Anal. Chem.* **1998**, *70*, 2881–2887.

(22) Martin, S. J.; Frye, G. C. *Appl. Phys. Lett.* **1990**, *57*, 1867–1869.

For the glycerol calibration, phase is assumed to be dependent only on viscoelastic changes in the sensing medium. Comparison of mass loadings of directly adsorbed species versus glycerol is used to illustrate the validity of this assumption. Protein adsorption of 150 and 250 ng/cm<sup>2</sup> (checked by SPR measurements) resulted in 23 and 34 deg acoustic phase changes, respectively. In the glycerol calibration of the same acoustic device, such mass per area loadings of glycerol in the sensing volume gave 1.5 and 2.4 deg change in phase, respectively. In the extreme case where all glycerol phase response is due to mass on the surface, an error of nearly 7% (2.4/34) would occur. Mass loading effects on SH-SAW phase have not been modeled other than for cases where pure elastic layers or very viscous layers attached directly to the sensing surface.<sup>13,23</sup> The fact that signal returns to its initial value when water is pumped over the device surface (Figure 2a) indicates that the glycerol is readily rinsed off. Since glycerol does not adsorb to the sensing surface, the results suggest that density changes arising from the glycerol mass are poorly sensed due to the differing nature of mass attachment to the sensing surface. To reduce this error in phase calibration, future calibrations may use solutions with constant density but with differing viscosity (e.g., poly(ethylene glycol) solutions of varying molecular weight) to obtain a purer viscoelastic phase response of each device.

Above, an empirical method using the acoustic response obtained for glycerol–water solutions is described in order to calibrate both the phase and amplitude response of the acoustic waveguide device. The viscoelastic information provided through amplitude response is used to determine the amount of phase response due to viscoelasticity. Linear response to glycerol–water solutions, or any other viscous series of solutions, is not necessary: any function used to relate amplitude change to properties of a viscous solution can be used in place of eq 1.

**Interpretation of Glycerol Equivalent Surface Viscosity,  $\eta_{\text{gly}}^s$ .** For any amplitude change occurring with a given device, correlation to an absolute viscosity of glycerol solution was made through the empirical glycerol calibration method. Absolute viscosity values include all relaxation mechanisms in material that occur on all time scales when a material is subjected to a shear force. Note that  $\eta_{\text{gly}}^s$  is not the absolute viscosity of the sensing volume: it represents an equivalent viscosity for only the relaxations sensed by the device. SAW devices sense relaxations with relaxation times only up to half the device wave period.<sup>13,19</sup> Wave periods for Q108 and Q155 devices are 6.5 and 9.6 ns, respectively. Therefore for all the measurements,  $\eta_{\text{gly}}^s$  includes viscoelasticity arising from relaxations only up to 3.2–4.8 ns. Note that a convenient method to measure viscoelasticity arising from relaxation mechanisms occurring at much higher relaxation time regimes is to work at a lower frequency. Future work could probe solutions of proteins by using devices with a larger disparity in frequency, i.e., 50 MHz versus 1 GHz, to resolve mechanisms occurring on the 1–20 ns time scale.

The glycerol calibration is used to obtain viscoelastic information,  $\eta_{\text{gly}}^s$ , about two biological systems, IgG bound to protein A and IgG adsorbed on Au. In the antibody deposition experiments, the surface of all devices were prepared and treated in the same manner in order to minimize any difference in antibody binding due to variations in surface morphology. Protein A, which is known to have a strong affinity for gold, was adsorbed on

the freshly prepared gold surface (data not shown) and used, subsequently, for binding different concentrations of IgG. Through the amplitude changes monitored during antibody deposition, the glycerol equivalent surface viscosities for the IgG–protein A complex and IgG adsorbed on Au were calculated by using eqs 2 and 3. Results for the glycerol equivalent surface viscosities ranges for IgG adsorbed on the Q155 gold surface, IgG–protein A complex on the Q108 surface, and IgG–protein A complex on the Q155 surface were 1.02–1.16, 1.03–1.23, and 1.04–1.30 cP, respectively.

In the  $\eta_{\text{gly}}^s$  representation, the viscosity change seen for any proteins on the surface is averaged over the sensing volume, whose thickness is frequency dependent through eq 10. Therefore as indicated by the above results, for measurement via the Q108 device the viscoelasticity of the layer is averaged over additional aqueous solution above the protein layer in comparison to measurements using the Q155 device whose sensing volume is thinner. The averaging over a larger volume for the same surface mass leads to a lower  $\eta_{\text{gly}}^s$  for Q108 measurements.

For the surface-localized protein layers, the measured glycerol equivalent surface viscosity is frequency dependent for another reason as well: the range of relaxation times in protein layers is larger than the device wave period (reciprocal of frequency). Previous work has established the range of relaxation times for proteins in solution to be 20–10<sup>6</sup> ns, and specifically for IgG in solution to be 504 ns.<sup>1</sup> Therefore through these devices that detect relaxations up to 4.8 ns, the sensed  $\eta_{\text{gly}}^s$  does not include the molecular relaxations of individual proteins and includes the faster relaxation process occurring over the protein layer. The viscoelasticity as probed by such SH-SAW devices in the 10<sup>2</sup>-MHz range will be different from similar work done on lower frequency devices such as quartz crystal microbalances.<sup>9</sup> Viscoelastic values from such lower frequency devices may include molecular rotations of proteins rather than the relaxation processes occurring over the extended protein layer. Information about molecular rotations is easily accessible through traditional hydrodynamic methods, while the later is rarely measured and is of interest.

Previous modeling of shear horizontal acoustic wave propagation in viscoelastic media have considered the media as homogeneous and having a single relaxation time.<sup>13,23</sup> All such modelings use a simple mechanical model for viscoelastic materials, the Maxwell model: a purely elastic spring and viscous dashpot connected in series. The empirically determined  $\eta_{\text{gly}}^s$  for protein layers can be interpreted as the viscosity of the dashpot. In such a treatment, the protein layer with a spectrum of relaxation times is reduced in the glycerol calibration to a homogeneous layer with a single relaxation time predicted by the glycerol calibration. Note that the Maxwell model assumes a uniform distribution of stress and cannot describe retarded elastic response of a material. More realistic predictions of viscoelastic behavior can be achieved by extending this rather simple model to include more elements with various characteristic viscosities with different characteristic relaxation times. More sophisticated calibrations must be used, however, for such modeling that enable resolution of different relaxation mechanisms. The empirical methods described in this work yield information that could fit well with current models<sup>14</sup> and could be the basis of future work.

**Surface Mass Coverage Calculation from Einstein Relation Modeling.** The viscoelastic effect of adding proteins to the surface of the acoustic waveguide device

(23) Wang, Z.; Cheeke, J. D. N.; Jen, C. K. *Appl. Phys. Lett.* **1994**, *64*, 2940–2942.

was modeled to be equivalent to adding solid particles to allow application of the Einstein relation (eq 5). In the model, the total volume of all particles perturbing the medium viscoelasticity is considered to be equivalent to the total volume of all protein molecules perturbing the viscoelasticity of the surface (Figure 3). From this powerful method, protein surface coverages are obtained (Figure 4). Modeling results for IgG–protein A binding mass coverage of 10–300 ng/cm<sup>2</sup> is in good agreement with literature values.<sup>9</sup> Maximum IgG–Au adsorption acoustic results (218 ng/cm<sup>2</sup>) are correctly below 695 ng/cm<sup>2</sup>, the maximum surface coverage based on computer simulations of processes similar to IgG adsorption.<sup>24</sup> The simulated coverage estimate takes into account the poor lateral mobility of adsorbed proteins: the simulation calculates the hole area on the surface in which additional IgG does not have enough space to adsorb onto after varying extents of random sequential adsorption. Validity of modeling with the Einstein relation has been tested by performing surface plasmon resonance (SPR) measurements of IgG adsorption to Au. Given a standard 15% deviation of SPR experimental surface mass results, very good correspondence between the two methods is seen (Figure 4). Similar adsorption results at 108 and 155 MHz (Figure 4) indicate that the model holds at two different frequencies. Therefore, the account for frequency dependence of the model via the penetration depth (eq 10) is valid.

Errors in surface coverage results arise primarily from the sensitivity of the model to molecular dimensions. Molecular dimensions are particularly sensitive to binding on surface, which is affected by flow regimes, surface roughness, pH, surface charge, etc.—all of which cannot be precisely controlled among all acoustic and SPR experiments. Crystallographic data are used to estimate the molecular dimensions of the adsorbed state of IgG. Since hydrodynamic estimates take into account intrinsic viscosity of proteins that are not measured with the device, such estimates were not used. For example, protein A dimensions calculated from hydrodynamic measurement or simulations (e.g., Stokes radius) yield molecular volumes 10 times larger than from specific volume estimates from amino acid sequence analysis. The model is also found to be sensitive for these data to the shape factor with maximum error of 29% between sphere ( $v = 2.5$ ) and prolate ellipsoid ( $v = 3.6$ ).

Linear phase response to mass deposition is predicted by theory<sup>25</sup> and is seen in these results. A pure phase response to mass (Figure 5) is obtained by correcting the total measured phase response to IgG with the glycerol calibration. The abscissa in Figure 5 is from modeling with the Einstein relation and the ordinate is the mass portion of phase response. The portion of phase change due to viscoelasticity is estimated as the phase change in Figure 2b for  $w_{\text{glyPrA}} + w_{\text{glyIgG}}$  during IgG binding or adsorption. Therefore the pure mass component of phase change during binding or adsorption is total measured phase change minus that predicted from glycerol calibration. Acoustoelectric interaction of IgG molecules is assumed to be negligible at the working pH and for the layered structure. Note that corresponding frequency changes can be easily obtained from the phase changes.

Nonlinearity in phase response at high surface concentration (Figure 5) is likely to be due to interactions between IgG antibodies, which has not been modeled. Each IgG molecule is modeled as a noninteracting particle of

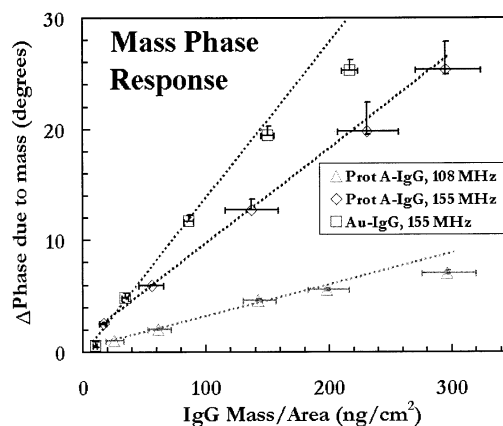


**Figure 5.** Acoustic phase response due to mass for mass deposition as predicted by modeling amplitude change. The viscoelastic component of the measured phase response was subtracted by using glycerol calibration. Ordinate error bars arise from random error in phase during binding or adsorption, while abscissa error bars arise from modeling the random error in amplitude during binding or adsorption.

equivalent volume. When IgG molecules are closely packed near the surface, the volume fraction of IgG may be larger than 0.2 (the cutoff criterion for the Einstein relation) in the local surface protein layer, even though the volume fraction of IgG in the thicker device sensing volume may be less than 0.2. For volume fractions greater than 0.2, mutual hindrance of particles or biomolecules by mutual obstruction of certain degrees of motion occurs. This hindrance causes deviation from the purely Brownian motion perturbation behavior of particles in a medium that Einstein characterizes through his relation. Therefore, the mechanical interaction between IgG molecules near the surface leads to viscoelasticity that cannot be adequately described by the Einstein relation. Nonlinearity in phase response can lead to such additional information about the mechanical interaction between closely packed IgG molecules. Furthermore, if IgG cross reactions occurred, the combined volume of the reacted complex generally would have decreased in comparison to that of two individual IgG molecules. This phenomenon would cause the surface coverage estimate to be too high, resulting in a negative deviation in Figure 5. At high surface coverages, cross reactivity is suggested and has been seen in the literature for IgG systems.<sup>21</sup> Future work with this model and sensor shows promise to yield information about cross reactivity as well.

## Conclusions

The viscoelasticity of surface protein layers was quantified in real time during the formation of the layer. Acoustic waveguide devices were used to sense such viscoelastic information, while monitoring mass changes in the layers simultaneously. A self-calibration technique for acoustic waveguide devices to separate empirically mass and viscoelastic response has been described. Via this technique, we have quantified viscoelastic response of biological layers as glycerol-equivalent surface viscosity. This viscosity yields comprehensive information about biological layer viscoelasticity averaged over a thin aqueous sensing volume (~50 nm thick) in a regime not probed by traditional viscoelastic detection techniques: the regime of relaxation processes in the biological layer with relaxation times up to half the device period (~5 ns). Modeling the viscosity through the Einstein relation for solid particles provided estimates of surface mass coverage for the protein layers. Evidence for interactions between

(24) Feder, J. J. *Theor. Biol.* **1980**, *87*, 237–254.

(25) Newton, M. I.; Martin, F.; Melzak, K.; Gizeli, E.; McHale, G. *Electron. Lett.* **2001**, *37*, 340–341.

the individual protein molecules at high surface coverages was seen.

**Acknowledgment.** We thank Dr. K. Melzak for fruitful discussions and Unipath for donating the anti-

bodies used in this work. Dr E. Gizeli and Mr K. Saha gratefully acknowledge the financial support of BBSRC and the US Winston Churchill Foundation.

LA026806P